

ORIGINAL ARTICLE

Spontaneous destructive periodontitis and skeletal bone damage in transgenic mice carrying a human shared epitope-coding *HLA-DRB1* allelePrashasnika Gehlot,¹ Sarah L Volk,² Hector F Rios,² Karl J Jepsen,³ Joseph Holoshitz¹

To cite: Gehlot P, Volk SL, Rios HF, *et al.* Spontaneous destructive periodontitis and skeletal bone damage in transgenic mice carrying a human shared epitope-coding *HLA-DRB1* allele. *RMD Open* 2016;**2**:e000349. doi:10.1136/rmdopen-2016-000349

► Prepublication history and additional material is available. To view please visit the journal (<http://dx.doi.org/10.1136/rmdopen-2016-000349>).

Received 22 August 2016

Accepted 8 November 2016



CrossMark

¹Departments of Internal Medicine, University of Michigan, Ann Arbor, Michigan, USA

²Departments of Periodontics and Oral Medicine, University of Michigan, Ann Arbor, Michigan, USA

³Departments of Orthopaedic Surgery, University of Michigan, Ann Arbor, Michigan, USA

Correspondence to

Dr Joseph Holoshitz;
Jholo@med.umich.edu

ABSTRACT

Objective: Shared epitope (SE)-coding *DRB1* alleles are associated with bone erosion in several diseases, including rheumatoid arthritis (RA) and periodontal disease (PD), but the underlying mechanism is unknown. We have recently identified the SE as an osteoclast-activating ligand. To better understand the biological effects of the SE in vivo, here we sought to determine whether it can facilitate spontaneous bone damage in naïve mice.

Methods: 3-month old naïve transgenic mice that carry the human SE-coding allele *DRB1**04:01, or a SE-negative allele *DRB1**04:02 were studied. Bone tissues were analysed by micro-CT, and the tooth-supporting tissues were studied by histology, immunohistochemistry and immunofluorescence. Serum biomarkers were determined by ELISA.

Results: Transgenic mice expressing the SE-coding *DRB1**04:01 allele, but not mice carrying the SE-negative allele *DRB1**04:02, showed spontaneous PD associated with interleukin (IL)-17 overabundance and periostin disruption. Mandibular bone volumetric and mineralisation parameters were significantly lower in SE-positive mice, and alveolar bone resorption was significantly increased in these mice. SE-positive mice also had more slender tibiae, and their marrow, cortical and total areas were lower than those of SE-negative mice. Additionally, significantly increased serum IL-17, tumour necrosis factor- α and osteoprotegrin levels were found in SE-positive mice, while their receptor activator of nuclear factor κ -B ligand levels were significantly lower.

Conclusions: A human SE-coding allele increases the propensity to spontaneous bone-destructive periodontal inflammation and skeletal bone damage in transgenic mice. These findings provide new insights into the previously documented but poorly understood association of the SE with accelerated bone erosion in RA and several other human diseases.

INTRODUCTION

Bone erosion is a devastating outcome in rheumatoid arthritis (RA) and periodontitis

Key questions

What is already known about this subject?

- The shared epitope (SE) is associated with several bone-damaging diseases, including rheumatoid arthritis (RA) and periodontal disease (PD).
- PD is more common in RA.
- Bone damage in RA affects both articular and extra-articular bone.
- Although PD is known to associate epidemiologically with RA, and both conditions associate with the SE, the pathogenic role of the SE is unknown.

What does this study add?

- Transgenic mice carrying a human SE-coding gene develop spontaneous, bone-destructive PD, implicating for the first time the SE as a direct pathogenic factor in PD.
- SE-positive mice also had slenderer tibiae, and their marrow, cortical and total areas were lower than those of SE-negative mice.
- Additionally, significantly increased serum interleukin-17, tumour necrosis factor- α and osteoprotegrin levels were found in SE-positive mice.
- These findings could provide new mechanistic insights into the previously documented but poorly understood association of the SE with bone erosion several diseases.
- The study could identify a new mechanism of RA–PD association.

How might this impact on clinical practice?

- Once translated to human systems, these findings could help design preventive, early diagnostic and therapeutic intervention modalities for bone damage-associated diseases, including, but not limited to, RA and PD.

(PD), two common diseases that co-associate epidemiologically.^{1–3} Although the molecular mechanism of the association is unknown, it

is worth noting that both conditions involve an interleukin (IL)-17-producing T helper (Th17) cell-dominated inflammatory process^{4 5} and osteoclast (OC)-mediated bone damage.^{6 7} Both RA⁸ and PD^{9 10} have been shown to associate with shared epitope (SE)-coding *HLA-DRB1* alleles. Cigarette smoking, which synergises with the SE to increase disease risk in RA,¹⁰ has been shown to increase PD risk as well.^{11 12} Additionally, protein citrullination, which closely associates with RA in SE-positive individuals¹³ has been purported to play a role in PD.¹⁴

We have recently identified the SE as a ligand that binds to cell surface calreticulin and activates pro-osteoclastogenic signalling.^{15–28} Using cell-free synthetic ligands expressing the SE motif, we have demonstrated that the SE enhanced Th17 polarisation²⁴ and directly activated OC differentiation.²⁶ When administered in vivo to mice with collagen-induced arthritis, the SE ligand enhanced joint inflammation, increased the abundance of tissue and bone marrow OCs, and enhanced bone damage in arthritic joints.^{23 25} Thus, the SE is a signal transduction ligand that contributes directly to bone destruction in a disease model of RA induced by antigen immunisation.

To investigate whether the SE ligand affect bone biology under physiological conditions as well, here we have undertaken to determine whether naïve transgenic mice expressing a SE-coding *HLA-DRB1* allele display bone abnormalities in two extra-articular areas of interest: jaws and tibiae. The findings indicate that SE-expressing mice display extensive bone-destructive PD along with skeletal bone abnormalities. These finding directly implicate the SE, for the first time, as a pathogenic factor in a spontaneous disease model, and suggest a potential new molecular mechanism for the well-documented but poorly understood higher incidence of erosive PD and diffuse skeletal bone damage in RA. The findings also provide a testable hypothesis concerning the reported association of the SE with bone damage in non-RA conditions.^{10 29 30}

MATERIALS AND METHODS

Animals

Tg mice, expressing SE-positive *HLA-DR4*04:01* or SE-negative *HLA-DR4*04:01* human alleles^{31 32} were kindly provided by Dr Chella David, at the Mayo Clinic, and are referred to as *DRB1*04:01* Tg and *DRB1*04:02* Tg mice, respectively. The two mouse strains have a mixed (predominantly B6) genetic background, which is ~99% identical between them. Experiments were carried out in 3-month-old male and female mice, weighing 19–25 g, housed in a specific pathogen-free, temperature-controlled room (25°C) with a 12-hour dark and 12-hour light cycle. A total of 20 naïve mice (no=5 in each group) were studied. Animals were allocated blindly to four experimental groups based solely on their gender and genotype. All protocols for mouse experiments were approved by the University of

Michigan Unit for Laboratory Animal Medicine and by the University of Michigan Committee on Use and Care of Animals. Mice were maintained in accordance with all applicable federal, state, local, and institutional laws, regulations, policies, principles and standards (including accreditation) governing animal research.

Micro-CT

Maxillae and mandibles

Hemimaxilla and hemimandible samples were formalin-fixed and examined by a micro-CT system (μ CT100 Scanco Medical, Bassersdorf, Switzerland) embedded in 1% agarose in a 34 mm diameter tube. The specimens were scanned with a voxel size of 18 μ m, and scan settings of 70 kVp, 114 μ A, 0.5 mm AL filter, and integration time 500 ms. To assess alveolar bone loss, the distances from the cemento enamel junction (CEJ) to the alveolar bone crest (ABC) were measured at four sites of second molars (mesiobuccal, distobuccal, mesiopalatal and distopalatal) in three-dimensional (3D) images viewed from buccal and palatal sides, with the assistance of the image analysis system (MicroView V.2.2 Advanced Bone Analysis Application, GE Healthcare Pre-Clinical Imaging, London, Ontario, Canada). Linear alveolar bone loss was determined by measuring the distances from the CEJ to the ABC were measured (interdental area between first and second molars). The measurements were repeated two times per site, and the results are presented as the distances in millimetres. To establish the residual amount of alveolar bone remaining in the interdental area between the first and second molar, the bone mineral density (BMD), bone volume fraction (BVf), bone mineral content (BMC), tissue mineral content (TMC) and tissue mineral density (TMD) were determined using a volumetric method, quantifying the structural bone based on microarchitectural parameters.

Tibiae

Specimens were scanned with a voxel size of 12 μ m, 70 kVp, 114 μ A, 0.5 mm AL filter and integration time 500 ms. The tibiae were reoriented with the mid-diaphysis parallel to the z-axis, and bone length was measured as the distance between the most proximal and distal transverse planes. Regions of interest (ROI) were located for cortical and trabecular parameters. A diaphyseal cortical ROI spanning 10% of total Tibia length was located midway between the distal growth plate and third trochanter. Parameters including cortical thickness, cross-sectional area, bending moment of inertia in the anterior–posterior direction, endosteal perimeter and periosteal perimeter were quantified with a commercially available software (MicroView V.2.2 Advanced Bone Analysis Application, GE Healthcare Pre-Clinical Imaging, London, Ontario, Canada).

A trabecular ROI covering 10% of total tibia length was located under the proximal growth plate. The inner cortical surface was defined with a splining algorithm. Trabecular metaphyseal bone was isolated with a more

conservative algorithm for each specimen based on the bimodal distribution between marrow and bone.³³ Parameters including marrow area, cortical area and total area were quantified using standard stereology algorithms (MicroView V2.2). A 3D sphere fitting algorithm was also used to confirm the stereology data for trabecular bone.³⁴

Immunohistochemistry

Tissues were fixed in 10% buffered formalin, decalcified, cut at 5 µm thickness, mounted on slides and air-dried at room temperature. Sections were deparaffinised, rehydrated and incubated with 3% hydrogen peroxide in methanol for 15 min at room temperature to eliminate endogenous peroxidase activity. Antigen retrieval was carried out at 95°C for 30 min by placing the slides in 0.01 M sodium citrate buffer (pH 6.0). The slides were then incubated with a primary rabbit polyclonal antibody for either IL-17A (Abcam #ab79056), periostin (Abcam #ab14041) or an isotype control (Abcam ab#27478) at 4°C overnight followed by secondary goat antirabbit (Abcam #ab6721). For immune detection, the avidin–biotin complex method was performed according to the manufacturer's instructions (TL-060-QHL—UltraVision Quanto Detection System HRP from Thermo Scientific). Colour development was achieved with 3, 3'-diaminobenzidine. Photographs were taken using an Olympus BX60 upright microscope.

Immunofluorescence

Slides were stained with a primary rabbit polyclonal antibody for IL-17 as above, followed by secondary donkey antirabbit IgG antibody conjugated to Alexa Fluor 594 (Abcam #ab150076) and stored at 4°C until use. DAPI (4', 6-diamidino-2-phenylindole, Sigma, #D9542) was used for nuclei staining. Quantification was carried out by a Biotek Cytation 5 instrument, using the Gen5Image + software (Biotek).

Quantification of serological biomarkers

Serum concentrations of osteoprotegerin (OPG), IL-6, receptor activator of nuclear factor κ-B ligand (RANKL), tumour necrosis factor (TNF)-α and IL-17 levels were analysed using Quantibody Mice Custom Array (RayBiotech, Norcross, Georgia, USA), according to the manufacturer's specifications. Each sample was assayed in quadruplicate. An Innoscan 710 with MAPIX software (Innopsys, Chicago, Illinois, USA) was used to determine fluorescence intensities.

Statistical analysis

Data analysis was performed with unpaired t-test, using a GraphPad Prism software V.6. All data are shown as mean±SEM. Statistical significance was defined as $p < 0.05$, and is denoted graphically as follows: * $p < 0.05$; ** $p < 0.005$; *** $p < 0.0005$.

RESULTS

Spontaneous PD in SE-expressing mice

Given the reported association between RA and PD^{1–3} and between these two diseases and the SE,^{9 10 35} we sought to determine whether the SE associates with spontaneous PD. To this end we examined 3 months old naïve Tg mice expressing the SE-coding *DRB1*04:01* allele, and compared them to control, naïve Tg mice expressing a non-SE-coding allele, *DRB1*04:02*.

Micro-CT-based 3D volumetric measurements (figure 1A) revealed a statistically significant bone loss in mandibles of SE-positive *DRB1*04:01* Tg male mice, compared with the SE-negative *DRB1*04:02* Tg control group. As shown, bone volume ($p = 0.008$), BVF ($p = 0.003$), BMD ($p = 0.0004$), BMC ($p = 0.002$), TMC ($p = 0.005$) and TMD ($p = 0.004$) were all significantly lower in SE-positive males, compared with SE-negative control male mice (figure 1A). In females, there were significant differences in TMD ($p = 0.0001$) and BMC ($p = 0.02$) between the SE-positive *DRB1*04:01* Tg and SE-negative *DRB1*04:02* groups, but not in other parameters (see online supplementary table SI).

In maxillae, there were significantly lower TMD readings in males ($p = 0.0009$) and females ($p = 0.02$) in the SE-positive *DRB1*04:01* Tg as compared with SE-negative *DRB1*04:02* Tg mouse groups, but not in other parameters (see online supplementary table SI). In 2D readings (see online supplementary table SII), male mandibles (figure 1B) and maxillae and female mandibles all showed higher linear distances between CEJ to the ABC in SE-positive *DRB1*04:01* Tg, as compared with SE-negative *DRB1*04:02* Tg mice; however, these differences did not reach statistical significance (see online supplementary table SII).

Histological examination of SE-positive Tg mice mandibles demonstrated increased periodontal inflammatory infiltrates, as compared with SE-negative Tg mice (figure 2A). Periostin is normally expressed in the periodontal ligament and other fibrous connective tissue³⁶ and plays a key role in maintaining periodontal stability in relation to tooth mechanical function.³⁷ Disruption of the periodontal ligament with irregular periostin is a common finding in PD. As can be seen in figure 2A, periodontal tissues of SE-positive *DRB1*04:01* Tg mice displayed disrupted periodontal ligaments as indicated by an irregular distribution of periostin. In contrast, in the SE-negative *DRB1*04:02* Tg mice periodontal tissues showed a well-organised ligament with normal distribution of periostin.

Immunohistochemistry staining for IL-17A showed higher abundance of the cytokine in SE-positive *DRB1*04:01* mice compared with SE-negative *DRB1*04:02* mice (figure 2B). Isotype-matched controls showed negative results, while a positive control tissue (inflammatory lymph node) showed strong staining (figure 2C). The overabundance of IL-17A in SE-positive mice was confirmed by immunofluorescence-based quantification (figure 2D). As can be seen, the

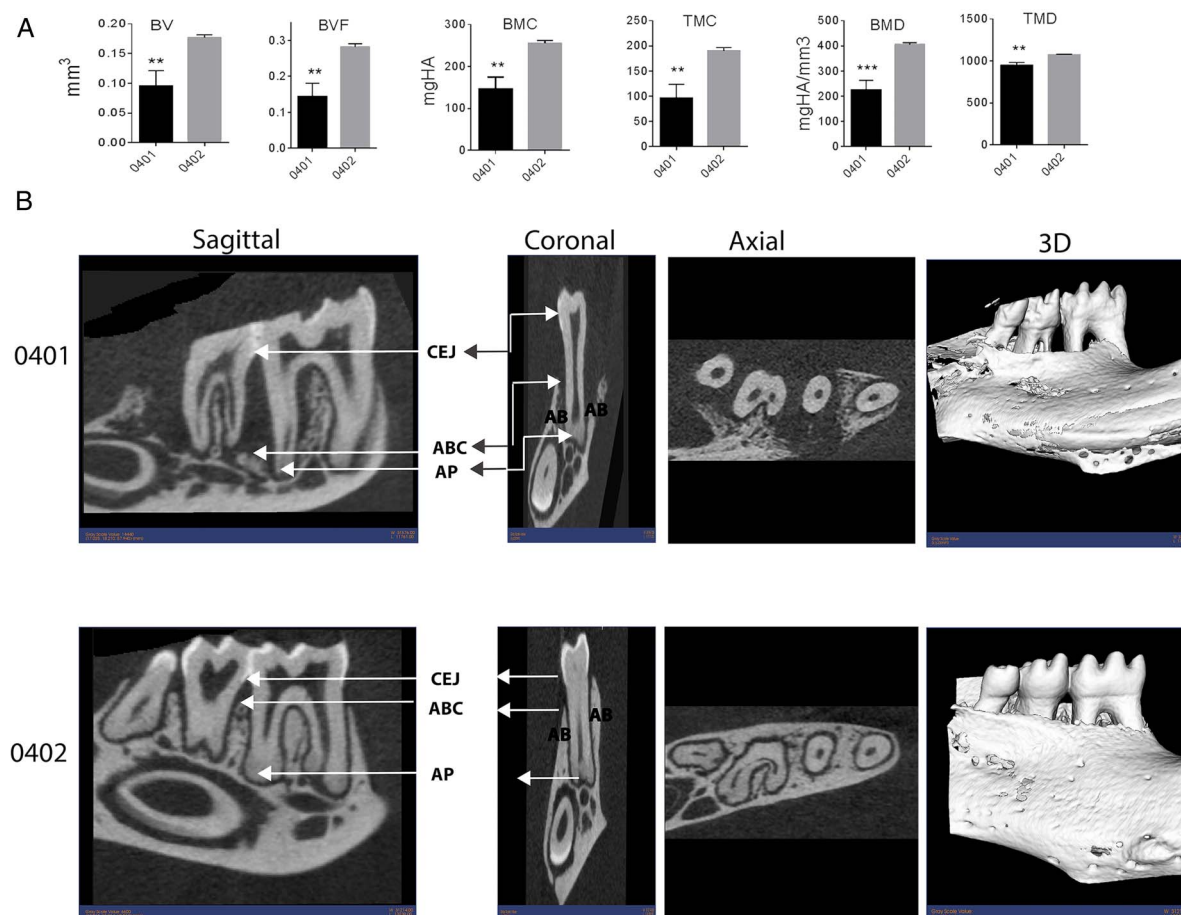


Figure 1 Periodontal micro-CT analyses. (A) 3D micro-CT-based quantification of mandibular bone parameters in SE-positive *DRB1*04:01* (black bars) and SE-negative *DRB1*04:02* (gray bars) Tg mice. Values represent mean and SEM (n=5 per group). (B) Sagittal, coronal and axial 2D (left 3 columns) and 3D (right column) micro-CT images of mandibles from representative SE-positive *DRB1*04:01* (upper panel) and SE-negative *DRB1*04:02* (lower panel) Tg male mice. 2D, two-dimensional; 3D, three-dimensional; ABC, alveolar bone crest; AP, anteroposterior; BV, bone volume; BMC, bone mineral content; BMD, bone mineral density; CEJ, cemento enamel junction; BVF, bone volume fraction; SE, shared epitope; TMC, tissue mineral content; TMD, tissue mineral density.

SE-positive *DRB1*04:01* Tg mice had a significantly higher percentage of IL-17A-expressing cells ($8.613 \pm 0.7410\%$) as compared with SE-negative *DRB1*04:02* Tg mice ($1.826 \pm 1.024\%$; $p < 0.0001$).

Long bone abnormalities in SE-positive mice

While SE-positive mice showed no spontaneous articular bone changes, they had profound long bone abnormalities. Representative tibial micro-CT images of SE-positive and SE-negative mice are shown in figure 3A. As table 1 specifies, total tibial area in SE-positive *DRB1*04:01* males ($0.65 \pm 0.03 \text{ mm}^2$) was $20.6 \pm 0.086\%$ lower than the area in SE-negative *DRB1*04:02* male group ($0.86 \pm 0.03 \text{ mm}^2$; $p = 0.004$). In SE-positive females, the total area ($0.63 \pm 0.01 \text{ mm}^2$) was $14.9 \pm 0.0026\%$ lower than in the SE-negative group ($0.74 \pm 0.02 \text{ mm}^2$; $p = 0.005$). SE-positive *DRB1*04:01* male tibiae also showed significantly reduced marrow ($p = 0.002$) and cortical ($p = 0.025$) areas compared with SE-negative *DRB1*04:02* males. In females, the

SE-positive *DRB1*04:01* group showed reduced tibial marrow ($p = 0.002$) and total areas ($p = 0.005$); however, the cortical area in females was not significantly different between SE-positive and SE-negative mice (table 1). Noteworthy, the differences between the SE-positive and SE-negative groups were not attributable to body mass differences, as weights did not differ significantly between SE-positive *DRB1*04:01* and SE-negative *DRB1*04:02* cohorts for either males or females (table 1). Different from the aforementioned differences, the trabecular bone was not affected by the mouse SE status (see online supplementary table SIII).

There was also a difference found in TMD between SE-positive and SE-negative mice. As figure 3B demonstrates, *DRB1*04:01* male tibiae showed significant lower TMD ($p = 0.0001$) in comparison to the SE-negative group. The female SE-positive group also showed significant lower in TMD ($p = 0.0441$) in comparison to the SE-negative group (figure 3B).

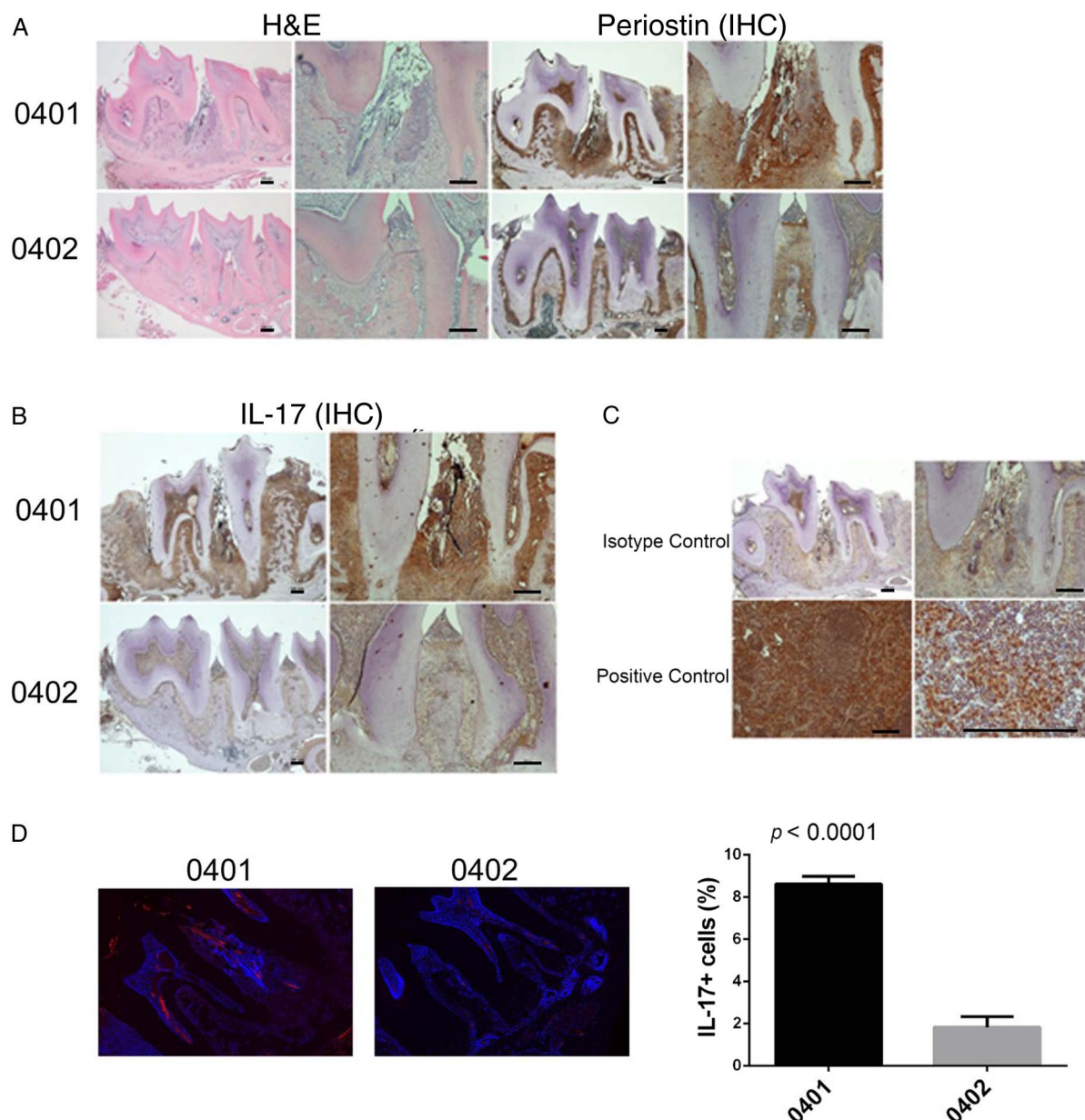


Figure 2 Spontaneous PD in *DRB1*04:01* mice. (A) Representative mandibular tissue sections stained with H&E (left) show intense inflammatory infiltrate (left). IHC staining for periostin (right) show disruption of the periodontal ligament in SE-positive, *DRB1*04:01* Tg mice (top panel). SE-negative *DRB1*04:02* Tg mice (bottom panel) show normal histology. (B) IHC staining for IL-17A showing markedly increased abundance of the cytokine in mandibular periodontal tissue of SE-positive, *DRB1*04:01* Tg mice (top panel), compared with SE-negative, *DRB1*04:02* Tg mice (bottom panel). (C) Isotype-matched antibody control shows negative IHC staining (top panel). A positive control tissue (draining lymph node—10 \times and 40 \times) shows the expected abundance of IL-17. In H&E and IHC, images of low (4 \times , left) and high (10 \times , right) magnification are shown. Horizontal bars represent 100 μ m. (D) Identification of IL-17-positive cells in periodontal tissues by immunofluorescence. Red fluorescence represents IL-17; blue fluorescence (DAPI) identifies nuclei. Boxed images show higher magnification images of regions identified by white arrows. Bar graph on the right depicts mean and SEM of IL-17-positive cells in SE-positive, *DRB1*04:01* Tg mice (black) and SE-negative, *DRB1*04:02* Tg mice (gray), as quantified by a Biotek Cytation5 instrument. DAPI, 4', 6-diamidino-2-phenylindole; IHC, immunohistochemistry; IL, interleukin; SE, shared epitope; PD, periodontal disease.

The SE status affected bone robustness as well. Robustness is defined as total cross-sectional area (Tt.Ar)/tibial length (Le) to be consistent with the fact that cross-sectional size increases proportional to the square of bone width (ie, area) during growth.³⁸ The

robustness (Tt.Ar/Le=total area) was found to be significantly lower in SE-positive males ($p=0.0018$) compared with the SE-negative control group, and a similar pattern was found in females ($p=0.0045$; figure 3C).

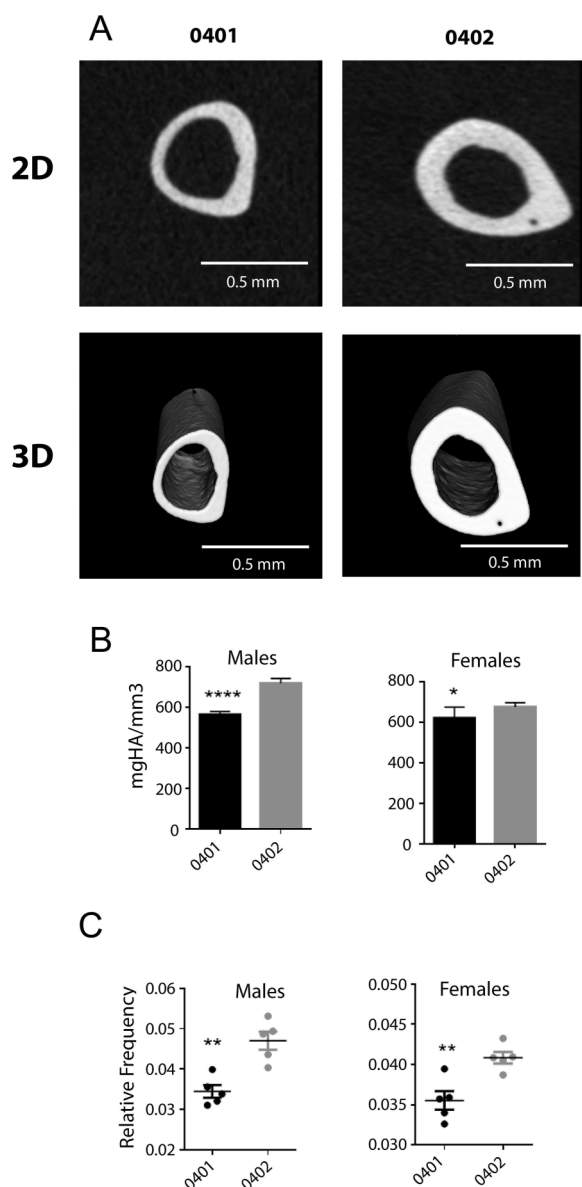


Figure 3 Tibial micro-CT analysis. (A) Representative 2D (upper panel) and 3D (lower panel) tibiae micro-CT images of SE-positive *DRB1*04:01* (left column) and SE-negative *DRB1*04:02* (right column) mice. (B) Tibial mineral density data of SE-positive *DRB1*04:01* (black bars) and SE-negative *DRB1*04:02* (gray bars) mice. (C) Male (left) and female (right) robustness data of the SE-positive *DRB1*04:01* (black dots) and SE-negative *DRB1*04:02* (gray dots) mouse groups. Values in (B) and (C) represent mean and SEM (n=5 per group). 2D, two-dimensional; 3D, three-dimensional; SE, shared epitope.

Serological markers

SE-positive and SE-negative mice differed in their serum cytokine levels (figure 4). As can be seen, TNF- α , IL-17 and OPG levels were all significantly higher in SE-positive *DRB1*04:01* compared with SE-negative *DRB1*04:02* mice (p=0.0148, 0.0253, and 0.0323, respectively). Interestingly, RANKL was significantly lower in SE-positive in comparison to SE-negative mice (p=0.03; figure 4).

DISCUSSION

This study demonstrates that Tg mice carrying a human SE-coding *HLA-DRB1*04:01* allele develop spontaneous erosive PD and skeletal cortical bone and marrow abnormalities, along with abnormal levels of inflammatory markers. The pathology is allele-specific, since no such aberrations were seen in control Tg mice carrying the *HLA-DRB1*04:02* allele, which codes a DR β chain that differs by only a few amino acid residues from the SE-positive chain. To the best of our knowledge, this is the first spontaneous disease model in SE-expressing Tg mice.

The SE, the most significant genetic risk factor for RA, was identified almost 30 years ago,⁸ but its functional role remains unclear. The prevailing hypothesis posits that the SE sequence, possibly together with one or two HLA-DR groove amino acid residues,^{39 40} may enable presentation of arthritogenic antigens to T cells. However, in addition to the fact that the identity of such putative antigen is unknown, the antigen presentation hypothesis as a sole aetiological basis for RA suffers from several additional important shortcomings, as discussed elsewhere.^{26 41}

In previous studies, we have demonstrated that the SE acts as a signal transduction ligand that facilitates Th17 and OC differentiation. When administered to mice with experimental arthritis, synthetic SE ligands, which are incapable of any antigen presentation, facilitated disease severity and increased Th17 polarisation and OC-mediated bone damage.^{23–25} Directly relevant to the present study, naïve Tg mice carrying the SE-coding allele *HLA-DRB1*04:01* showed higher propensity to osteoclastogenesis and bone degradation activity *ex vivo*.^{24 25} Thus, our previous studies indicate that independent of its putative role in antigen presentation, the SE may contribute directly to arthritis severity as a signal transduction ligand that facilitates an OC-mediated bone-destructive pathway.

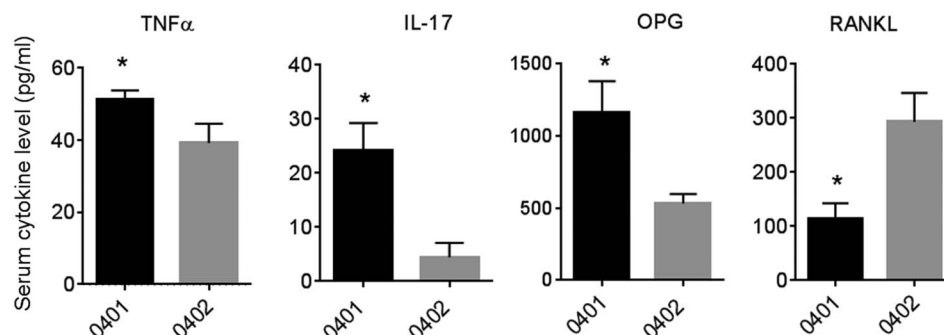
The findings of this study lend support to a bone remodelling effect of the SE ligand in physiological conditions as well. As shown here, SE-expressing mice spontaneously developed severe Th17-dominated PD, associated with bone destruction. This happened without intentional exposure to any infectious, chemical or mechanical stimuli. The fact that the pathology found here was limited to extra-articular bone, while joint tissues were spared, suggests that a specific immune response to joint antigens is unlikely to be the underlying mechanism of the SE effect in these mice.

It is noteworthy that PD and RA have been previously found to co-associate.^{1–3} One of the hypotheses postulates that PD-associate pathogenic bacteria, such as *Porphyromonas gingivalis* may be the culprit, due to their ability to facilitate protein citrullination.⁴² However, conclusive evidence to substantiate this cause–effect relationship is yet to be found. The findings of this study suggest that irrespective of whether such putative cause–effect scenario plays a role, the SE facilitates widespread bone damage processes.

Table 1 Tibiae–cortical bone parameters

Group	Total area (mm ²)	p Value	Cortical area (mm ²)	p Value	Marrow area (mm ²)	p Value	Weight (grams)	p Value
Males								
0401	0.67±0.07	0.003	0.42±0.08	0.025	1.83±0.02	0.001	24.96±1.14	0.081
0402	0.85±0.08		0.52±0.05		2.21±0.03		26.24±0.87	
Females								
0401	0.63±0.02	0.004	0.37±0.01	0.649	1.89±0.01	0.001	19.24±0.82	0.135
0402	0.74±0.05		0.37±0.02		2.24±0.04		21.04±2.28	

Figure 4 Serological markers. Serum concentrations of TNF- α , IL-17, RANKL and OPG in SE-positive *DRB1*04:01* (black bars) and SE-negative *DRB1*04:02* (gray bars) mice. Values represent mean and SEM (n=5 per group). IL, interleukin; OPG, osteoprotegerin; RANKL, receptor activator of nuclear factor κ -B ligand; SE, shared epitope; TNF, tumour necrosis factor.



The bone effects of the SE extended beyond the periodontal site and included skeletal tissues. The reduced tibial total area in SE-positive mice suggests suppression of periosteal expansion during growth. This effect was seen in both sexes, albeit slightly more severe in males. The reduced cortical area in the males, but not females, suggests sex difference in mass accumulation. Additional studies examining mice at multiple time points are warranted to determine whether the reduced mass in males was a result of altered bone growth or excessive resorption (loss). The mechanism of SE-associated reduced periosteal expansion is unclear, but may be linked to our previous findings of OC activation and proinflammatory effects of the SE ligand. Together, the reduced external size, cortical mass and robustness would suggest that similar to patients with RA,^{43–44} SE-positive mice might have reduced bone strength.

It has been previously found that bone damage in RA involves articular, periarticular and systemic skeletal tissues.⁴⁵ The reasons for this widespread bone damage are unclear. In this study, we demonstrated substantial skeletal bone damage in SE-expressing Tg mice. This finding may suggest that the pathogenesis of skeletal bone damage in this disease might be, at least partly, genetically determined by the SE ligand effect, rather than solely due to inflammation, as is commonly postulated.

Although SE-associated PD and bone pathology affected both male and female mice, there was a slightly greater predilection for such effects in males. The reasons for this apparent gender-biased effect are presently unclear. The trends were similar in both genders, but we cannot rule out that sex hormones may have a

direct contributory role. Alternatively, the observed gender-associated differences could be related to secondary gender-associated factors. For example, gender-associated mechanical factors, such as body mass, mobility or mastication differences between males and female could have partially contributed to the observed differences. Further research is required to better determine whether and why PD and skeletal damage are disparately affecting male and female SE-expressing Tg mice.

Consistent with the previously documented proinflammatory effects of the SE ligand^{17–23–25} in this study we demonstrate that Tg mice expressing the SE-coding allele had higher constitutive serum levels of TNF- α and IL-17. Additionally, periodontal tissues in SE-positive mice displayed a significant overabundance of IL-17-positive cells in situ. Counterintuitively however, RANKL levels were lower, and OPG levels were higher in SE-positive mice. The reason for this finding is unknown; however, it may be consistent with our previous observations that SE ligand-activated OC differentiation is RANKL-independent, as the SE ligand could induce such differentiation even in the absence of RANKL,²⁵ and our recent transcriptome analyses suggest that SE-activated and RANKL-activated osteoclastogenesis are mediated by substantially non-overlapping pathways (unpublished). Thus, it is tempting to speculate that the observed increased OPG levels in SE-expressing Tg mice might signify a defence response to other, RANKL-independent biochemical cues of excessive bone damage.

Finally, it should be noted that gut microbiota of SE-positive *DRB1*04:01* Tg and SE-negative *DRB1*04:02* Tg mice have been previously shown to differ.⁴⁶

Whether or how such a purported difference could affect the findings of the present study is open to speculations. One future approach to answering this question would be to determine whether microbiota from susceptible, SE-positive *HLA-DRB1*04:01* mice can transfer the bone phenotype to resistant, SE-negative *HLA-DRB1*04:02* mice. Be that as it may, our previous studies have shown that the SE ligand directly activates OC-mediated bone damage in vitro in cell lines, independent of microbiota or other in vivo, strain-dependent or environmental influences.

In summary, we demonstrate here that Tg mice expressing a SE-coding *HLA-DRB1* allele develop spontaneous erosive PD, skeletal abnormalities and serological evidence of a systemic inflammatory state. Molecular characterisation of the mechanisms involved could advance our understanding of the impact of the SE on bone remodelling in health and disease.

Acknowledgements JH has been supported by the Eleanor and Larry Jackier Research Award from the University of Michigan—Israel Partnership for Research programme, and by grants from The National Institute of Dental and Craniofacial Research (R21 DE023845) and The National Institute of Arthritis and Musculoskeletal and Skin Diseases (R01AR059085).

Contributors PG and SLV conducted experiments and acquired data. PG, HFR, KJJ and JH designed the research study, analysed data and wrote the manuscript.

Funding Eleanor and Larry Jackier Research Award from the UM—Israel Partnership for Research programme and by grants The National Institute of Dental and Craniofacial Research (R21 DE023845) and The National Institute of Arthritis and Musculoskeletal and Skin Diseases (R01AR059085).

Disclaimer The content is solely the responsibility of the authors and does not necessarily represent the official views of the National Institutes of Health.

Competing interests None declared.

Ethics approval All protocols for mouse experiments were approved by the University of Michigan Unit for Laboratory Animal Medicine and by the University of Michigan Committee on Use and Care of Animals.

Provenance and peer review Not commissioned; externally peer reviewed.

Data sharing statement No additional data are available.

Open Access This is an Open Access article distributed in accordance with the Creative Commons Attribution Non Commercial (CC BY-NC 4.0) license, which permits others to distribute, remix, adapt, build upon this work non-commercially, and license their derivative works on different terms, provided the original work is properly cited and the use is non-commercial. See: <http://creativecommons.org/licenses/by-nc/4.0/>

REFERENCES

- Mercado FB, Marshall RI, Klestov AC, *et al.* Relationship between rheumatoid arthritis and periodontitis. *J Periodontol* 2001;72:779–87.
- de Pablo P, Chapple IL, Buckley CD, *et al.* Periodontitis in systemic rheumatic diseases. *Nat Rev Rheumatol* 2009;5:218–24.
- da Silva AP, Bissada NF. “Arthritis and Periodontitis: an association debated for over two centuries”. *Curr Rheumatol Rev* Published Online First: 26 Oct 2015.
- Miossec P, Korn T, Kuchroo VK. Interleukin-17 and type 17 helper T cells. *N Engl J Med* 2009;361:888–98.
- Gaffen SL, Hajishengallis G. A new inflammatory cytokine on the block: re-thinking periodontal disease and the Th1/Th2 paradigm in the context of Th17 cells and IL-17. *J Dent Res* 2008;87:817–28.
- Fujikawa Y, Shingu M, Torisu T, *et al.* Bone resorption by tartrate-resistant acid phosphatase-positive multinuclear cells isolated from rheumatoid synovium. *Br J Rheumatol* 1996;35:213–17.
- Wiebe SH, Hafezi M, Sandhu HS, *et al.* Osteoclast activation in inflammatory periodontal diseases. *Oral Dis* 1996;2:167–80.
- Gregersen PK, Silver J, Winchester RJ. The shared epitope hypothesis. An approach to understanding the molecular genetics of susceptibility to rheumatoid arthritis. *Arthritis Rheum* 1987;30:1205–13.
- Bonfil JJ DF, Mercier P, Revirion D, *et al.* A “case control” study on the role of HLA DR4 in severe periodontitis and rapidly progressive periodontitis. Identification of types and subtypes using molecular biology (PCR-SSO). *J Clin Periodontol* 1999;26:77–84.
- Marotte H, Farge P, Gaudin P, *et al.* The association between periodontal disease and joint destruction in rheumatoid arthritis extends the link between the HLA-DR shared epitope and severity of bone destruction. *Ann Rheum Dis* 2006;65:905–9.
- Javed F, Al-Askar M, Samaranyake LP, *et al.* Periodontal disease in habitual cigarette smokers and nonsmokers with and without prediabetes. *Am J Med Sci* 2013;345:94–8.
- Källberg H, Ding B, Padyukov L, *et al.* Smoking is a major preventable risk factor for rheumatoid arthritis: estimations of risks after various exposures to cigarette smoke. *Ann Rheum Dis* 2011;70:508–11.
- Huizinga TW, Amos CI, van der Helm-van Mil AH, *et al.* Refining the complex rheumatoid arthritis phenotype based on specificity of the HLA-DRB1 shared epitope for antibodies to citrullinated proteins. *Arthritis Rheum* 2005;52:3433–8.
- Lundberg K, Wegner N, Yucel-Lindberg T, *et al.* Periodontitis in RA—the citrullinated enolase connection. *Nat Rev Rheumatol* 2010;6:727–30.
- Ling S, Lai A, Borschukova O, *et al.* Activation of nitric oxide signaling by the rheumatoid arthritis shared epitope. *Arthritis Rheum* 2006;54:3423–32.
- Ling S, Li Z, Borschukova O, *et al.* The rheumatoid arthritis shared epitope increases cellular susceptibility to oxidative stress by antagonizing an adenosine-mediated anti-oxidative pathway. *Arthritis Res Ther* 2007;9:R5.
- Ling S, Pi X, Holoshitz J. The rheumatoid arthritis shared epitope triggers innate immune signaling via cell surface calreticulin. *J Immunol* 2007;179:6359–67.
- Ling S, Cheng A, Pumpens P, *et al.* Identification of the rheumatoid arthritis shared epitope binding site on calreticulin. *PLoS ONE* 2010;5:e11703.
- Holoshitz J, Ling S. Nitric oxide signaling triggered by the rheumatoid arthritis shared epitope: a new paradigm for MHC disease association? *Ann N Y Acad Sci* 2007;1110:73–83.
- Holoshitz J, De Almeida DE, Ling S. A role for calreticulin in the pathogenesis of rheumatoid arthritis. *Ann N Y Acad Sci* 2010;1209:91–8.
- de Almeida DE, Ling S, Holoshitz J. New insights into the functional role of the rheumatoid arthritis shared epitope. *FEBS Lett* 2011;585:3619–26.
- Ling S, Cline EN, Haug TS, *et al.* Citrullinated calreticulin potentiates rheumatoid arthritis shared epitope signaling. *Arthritis Rheum* 2013;65:618–26.
- Fu J, Ling S, Liu Y, *et al.* A small shared epitope-mimetic compound potentially accelerates osteoclast-mediated bone damage in autoimmune arthritis. *J Immunol* 2013;191:2096–103.
- de Almeida DE, Ling S, Pi X, *et al.* Immune dysregulation by the rheumatoid arthritis shared epitope. *J Immunol* 2010;185:1927–34.
- Holoshitz J, Liu Y, Fu J, *et al.* An HLA-DRB1-coded signal transduction ligand facilitates inflammatory arthritis: a new mechanism of autoimmunity. *J Immunol* 2013;190:48–57.
- de Almeida DE, Holoshitz J. MHC molecules in health and disease: at the cusp of a paradigm shift. *Self Nonself* 2011;2:43–8.
- Naveh S, Tal-Gan Y, Ling S, *et al.* Developing potent backbone cyclic peptides bearing the shared epitope sequence as rheumatoid arthritis drug-leads. *Bioorg Med Chem Lett* 2012;22:493–6.
- Ling S, Liu Y, Fu J, *et al.* Shared epitope-antagonistic ligands: a new therapeutic strategy in mice with erosive arthritis. *Bioorg Med Chem Lett* 2015;67:2061–70.
- Korendowych E, Dixey J, Cox B, *et al.* The Influence of the HLA-DRB1 rheumatoid arthritis shared epitope on the clinical characteristics and radiological outcome of psoriatic arthritis. *J Rheumatol* 2003;30:96–101.
- Chan MT, Owen P, Dunphy J, *et al.* Associations of erosive arthritis with anti-cyclic citrullinated peptide antibodies and MHC Class II alleles in systemic lupus erythematosus. *J Rheumatol* 2008;35:77–83.
- Pan S, Trejo T, Hansen J, *et al.* HLA-DR4 (DRB1*0401) transgenic mice expressing an altered CD4-binding site: specificity and

- magnitude of DR4-restricted T cell response. *J Immunol* 1998;161:2925–9.
32. Taneja V, Taneja N, Behrens M, *et al.* HLA-DRB1*0402 (DW10) transgene protects collagen-induced arthritis-susceptible H2Aq and DRB1*0401 (DW4) transgenic mice from arthritis. *J Immunol* 2003;171:4431–8.
 33. OTSU N. A threshold selection method from gray-level histograms. *IEEE Trans Syst Man Cybern* 1979;9:62–6.
 34. Hildebrand TR, R  egsegger P. A new method for the model-independent assessment of thickness in three-dimensional images. *J Microscopy (Oxford)* 1997;185:167–75.
 35. Holoshitz J. The rheumatoid arthritis HLA-DRB1 shared epitope. *Curr Opin Rheumatol* 2010;22:293–8.
 36. Romanos GE, Asnani KP, Hingorani D, *et al.* PERIOSTIN: role in formation and maintenance of dental tissues. *J Cell Physiol* 2014;229:1–5.
 37. Rios HF, Ma D, Xie Y, *et al.* Periostin is essential for the integrity and function of the periodontal ligament during occlusal loading in mice. *J Periodontol* 2008;79:1480–90.
 38. Jepsen KJ, Courtland HW, Nadeau JH. Genetically determined phenotype covariation networks control bone strength. *J Bone Miner Res* 2010;25:1581–93.
 39. Raychaudhuri S, Sandor C, Stahl EA, *et al.* Five amino acids in three HLA proteins explain most of the association between MHC and seropositive rheumatoid arthritis. *Nat Genet* 2012;44:291–6.
 40. Kim K, Jiang X, Cui J, *et al.* Interactions between amino acid-defined major histocompatibility complex class II variants and smoking in seropositive rheumatoid arthritis. *Nat Genet* 2015;67:2611–23.
 41. Holoshitz J. The quest for better understanding of HLA-disease association: scenes from a road less travelled by. *Discov Med* 2013;16:93–101.
 42. Liao F, Li Z, Wang Y, *et al.* Porphyromonas gingivalis may play an important role in the pathogenesis of periodontitis-associated rheumatoid arthritis. *Med Hypotheses* 2009;72:732–5.
 43. van Staa TP, Geusens P, Bijlsma JW, *et al.* Clinical assessment of the long-term risk of fracture in patients with rheumatoid arthritis. *Arthritis Rheum* 2006;54:3104–12.
 44. Malgo F, Appelman-Dijkstra NM, Termaat MF, *et al.* High prevalence of secondary factors for bone fragility in patients with a recent fracture independently of BMD. *Arch Osteoporos* 2016;11:12.
 45. de Punder YM, van Riel PL. Rheumatoid arthritis: understanding joint damage and physical disability in RA. *Nat Rev Rheumatol* 2011;7:260–1.
 46. Gomez A, Luckey D, Yeoman CJ, *et al.* Loss of sex and age driven differences in the gut microbiome characterize arthritis-susceptible 0401 mice but not arthritis-resistant 0402 mice. *PLoS ONE* 2012;7:e36095.